Reaching Sachdev-Ye-Kitaev physics by shaking the Hubbard model

Charles Creffield [1,*] Fernando Sols [1] Marco Schirò,[2] and Nathan Goldman [3,4,†]

[1] Departamento de Física de Materiales, Universidad Complutense de Madrid, E-28040 Madrid, Spain
[2] JEIP, UAR 3573 CNRS, Collège de France, PSL Research University,
11 Place Marcelin Berthelot, 75321 Paris Cedex 05, France
[3] Laboratoire Kastler Brossel, Collège de France, CNRS, ENS-Université PSL,
Sorbonne Université, 11 Place Marcelin Berthelot, 75005 Paris, France
[4] International Solvay Institutes, 1050 Brussels, Belgium

(Dated: December 3, 2025)

The Sachdev-Ye-Kitaev (SYK) model has attracted widespread attention due to its relevance to diverse areas of physics, such as high temperature superconductivity, black holes, and quantum chaos. The model is, however, extremely challenging to realize experimentally. In this work, we show how a particular form of Floquet engineering, termed "kinetic driving", effectively eliminates single-particle processes and creates quasi-random all-to-all interactions when applied to models of Hubbard type. For the specific case of the Bose-Hubbard model, we explicitly verify that the driven system indeed reproduces SYK physics by direct comparison of the spectral form factor and out-of-time ordered correlation functions (OTOCs). Our findings indicate that a cold-atom realization of kinetic driving – achieved through modulation of hopping amplitudes in an optical lattice – offers a practical and accurate platform for quantum simulation of the SYK model.

Introduction — The Sachdev-Ye-Kitaev (SYK) model [1, 2] has become a topic of intense theoretical interest in recent years. The model describes random, all-to-all interactions between fermions, where the particles move collectively in pairs with no single-particle hopping processes. A consequence of its extremely dense low-energy spectrum is that the SYK model lacks quasiparticle excitations, making it a natural candidate to describe non-Fermi liquid physics. Its applications range [3] from modeling the strange metal phase in high temperature superconductors, to holographic quantum matter and information scrambling in black holes, and it has become a paradigmatic system for the study of extreme many-body quantum chaos. Its solvability in the large-N limit, where N is the number of fermion flavors, thus provides an attractive way of exploring these phenomena in a tractable manner. The bosonic version of the SYK model has received considerably less attention. While the bosonic representation is known to display different low-temperature physics, notably with a glassy phase with replica symmetry breaking, its high-energy properties share much of the features of its fermionic counterpart [4–9].

Despite the model's simplicity from a theoretical point of view, the complicated long-range nature of the interactions makes it extremely challenging to realize experimentally. Various suggestions have been made for solid-state implementations such as a graphene flake with an irregularly shaped boundary [10], or by using Majorana modes hosted by superconducting wires [11] or the surface of a topological insulator [12]. The excellent controllability of ultracold atoms held in optical lattice potentials also provides an appealing pathway towards simulating the SYK model [13, 14], with Rydberg arrays [15] and cavity-QED systems [16, 17] offering similar advantages. Digital quantum circuits have been proposed too [18, 19], and small-scale implementations of SYK systems have been achieved recently on Google's Sycamore [20] and IBM quantum processors [21, 22].

An alternative approach to developing complicated laboratory experiments is to *engineer* the required interactions by using a Floquet approach, and driving a relatively simple system. In the Floquet technique, a parameter of the system is varied periodically, and in the high-frequency regime the system can then be described by an effective static Hamiltonian, consisting of terms that have been renormalized or created by the driving. In principle, these various terms can be calculated perturbatively through the inverse-frequency or Magnus expansions [23–26]. A well-known example of this type of engineering is the periodically-driven Bose-Hubbard model. By oscillating the lattice potential – "shaking" the system – the tunneling can be tuned to zero, allowing the Mott transition to be dynamically controlled [27]. More complicated driving schemes can be devised to produce complex tunneling elements [28–34], allowing driven systems to emulate synthetic gauge fields and topological band structures [35–37]. Beyond the control over single-particle properties, Floquet engineering can also be used to effectively create complex interaction processes, including multi-body interactions [38–41], correlated hopping [42–48], pair hopping [49–51], spin-spin interactions [52–56], and chiral p-wave pairing [57].

In this work, we employ a driving protocol known as "kinetic driving" [58–60], in which the kinetic energy term of a system is periodically modulated such that its time-averaged value vanishes. When this driving is applied to a

* c.creffield@fis.ucm.es
† nathan.goldman@lkb.ens.fr

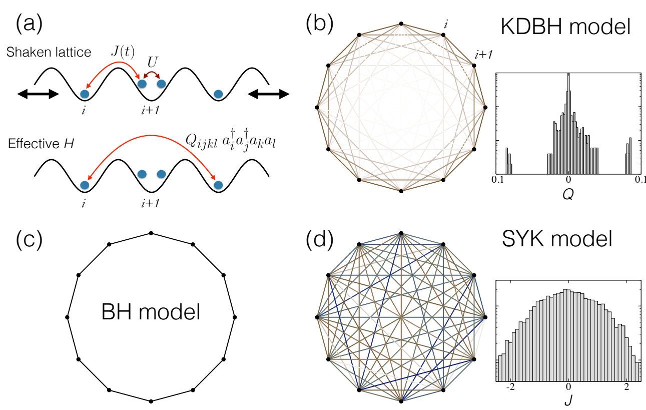

FIG. 1. (a) Particles held in an optical lattice can be well described by the Hubbard model (Eq. (1)), with nearest neighbor hopping J and onsite repulsion U. Shaking the lattice allows us to make J a time periodic function At high driving frequencies this produces a static effective model with long-ranged interaction terms of the form $Q_{ijkl}a_i^\dagger a_j^\dagger a_k a_l$ describing processes like doublon hopping and assisted tunneling. (b) Schematic representation of the interaction amplitudes of the KDBH model (Eq. 2) shaded according to their magnitude, $|Q_{ijkl}|$. The strongest links are between nearest neighbors, and their magnitude falls as the distance between the sites increases. Inset: The cumulative distribution of Q_{ijkl} for $0.6 \le \kappa \le 0.9$, where κ is sampled in steps of 0.01. The histogram is plotted on a logarithmic scale. The distribution is strongly peaked at small Q, and unlike the distribution of the SYK model, has gaps. (c) In the Bose-Hubbard model a given site i is only connected to its nearest-neighbors by single-particle tunneling processes. (d) As in (b) but for the SYK model (Eq. 3). Every site is connected to every other site by a random tunneling amplitude. Inset: In contrast the the effective model, the distribution of the amplitudes $J_{ij;kl}$ is dense and is of Gaussian form, so that when plotted logarithmically the histogram is parabolic.

Hubbard-type lattice model, the resulting effective Hamiltonian simplifies to a sum of all-to-all quartic interaction terms of the form $Q_{ijkl}a_i^\dagger a_j^\dagger a_k a_l$, characterized by a broad distribution of coupling strengths – closely resembling the structure of the SYK model; see Fig. 1(a). As the general form of the effective interactions does not depend on the statistics of the particles, our method equally applies to fermionic and bosonic Hubbard models. For concreteness, we restrict our numerical studies to the case of the Bose-Hubbard (BH) model, and term the resulting effective model the "kinetically-driven Bose-Hubbard" (KDBH) model. We explicitly validate the relation of the KDBH model to the bosonic SYK model by comparing their spectral form functions and out-of-time ordered correlation functions (OTOCs), using exact diagonalization methods. In this way, we also investigate the behavior of the bosonic SYK model, which in contrast to the fermionic case, has remained largely unexplored so far [4–9]. Our proposed scheme offers a practical route for the experimental exploration of SYK-type models in optical-lattice setups, where kinetic driving can be implemented by simply shaking the lattice [26, 37, 58].

Model — We begin with the Bose-Hubbard (BH) model [61, 62] describing bosonic particles, moving on a 1D lattice

$$H = -J\sum_j \left(b_j b_{j+1}^\dagger + \text{H.c.}\right) + U\sum_j b_j^\dagger b_j^\dagger b_j b_j \ , \qquad (1)$$

where $b_j/b_j^\dagger$ are bosonic annihilation / creation operators acting on lattice site j. The model includes two processes: nearest-neighbor hopping parameterized by the hopping amplitude J, and the onsite Hubbard repulsion U; see the sketch in Fig. 1(a). For periodic boundary conditions, H can be represented graphically as shown in Fig. 1(c), where each site is simply linked by J to its nearest neighbors. We emphasise that the approach described below can also be readily applied to spinless fermions, in which case the bare interaction terms act between nearest-neighbor sites; see End Matter for a study of the fermionic case.

Following Ref. [58], we now consider shaking the lattice such that $J \to J(t)$ varies periodically with time. Importantly, we require that its time-average is zero over a driving period. By making the particular choice $J(t) = J_0 \cos\omega t$, one can obtain an expression for the effective Hamiltonian in the high-frequency limit $\omega \gg U$, corresponding to the lowest-order term in the Magnus expansion [23–26]. For the Bose-Hubbard model in Eq. (1), the effective Hamiltonian takes the form

$$H_{\text{KDBH}} = U\sum_{i,j,k,l} Q_{ijkl}\, b_i^\dagger b_j^\dagger b_k b_l \ , \qquad (2)$$

where the interaction amplitudes Q_{ijkl} depend on the driving parameters; see the End Matter for a derivation of the effective Hamiltonian, in both the bosonic and fermionic cases. Importantly, the single-particle hopping processes present in the undriven Hubbard Hamiltonian H have been eliminated by the drive, as required for realizing a SYK-type model. In fact, since the hopping energy scale J has disappeared from the problem, the bare interaction strength U now simply enters as an overall energy scale. Henceforth, without loss of generality, we set $U = 1$.

We now compare the obtained KDBH Hamiltonian with the target (bosonic) SYK model. We restrict ourselves to considering the real variant of the model,

$$H_{\text{SYK}} = \sum_{i,j,k,l} J_{ij;kl}\, b_i^\dagger b_j^\dagger b_k b_l \ , \qquad (3)$$

where $J_{ij;kl}$ are real random variables sampled from a Gaussian distribution with zero mean and unit variance, and which satisfy bosonic exchange statistics and Hermiticity,

$$J_{ij;kl} = J_{ji;kl} = J_{ij;lk} = J^*_{kl;ij} \ . \qquad (4)$$

As shown in Fig. 1(d), these interaction terms link every site to every other site, the amplitude of each link being a random number.

Examining $H_{\rm KDBH}$ immediately reveals that it has the same structure of 4-operator terms as $H_{\rm SYK}$, and that the conditions (4) are automatically satisfied by the amplitudes Q_{ijkl}. The two Hamiltonians only differ in that the Q_{ijkl} are not random, but depend in a somewhat complicated way on the ratio of driving parameters, $\kappa = J_0/\omega$; see End Matter. Although in principle these amplitudes can be long-ranged, in practice they do fall as the separation between the site indices increases. This produces the situation depicted in Fig. 1(b), which is intermediate between the BH and the SYK cases. Clearly the connectivity of the lattice is much higher than the BH case, but the smallness or absence of some of the Q_{ijkl} amplitudes means that the $H_{\rm KDBH}$ is considerably more sparse than $H_{\rm SYK}$.

Sparse versions of the SYK model have been studied previously [63, 64], and it has been concluded that they continue to reproduce SYK physics as long as more than $\sim 10\%$ of the matrix elements of the Hamiltonian are non-zero. As $H_{\rm KDBH}$ has a sparsity of about 50% (that is, approximately half the terms of the Hamiltonian are either zero or negligibly small) this condition is amply fulfilled in our case. As illustrated in Fig. 1(b), we find that the distribution of the amplitudes differs from the dense Gaussian distribution of the SYK model. We will see, however, that these twin effects, the sparsity of the Hamiltonian and the non-Gaussian distribution of the amplitudes, do not prevent $H_{\rm KDBH}$ from emulating the SYK model with excellent fidelity.

Results — To investigate how closely the KDBH model reproduces SYK physics, we will first consider its chaoticity. A commonly used probe of quantum chaos is the distribution of spectral spacings. According to the Berry-Bohigas conjecture, integrable systems will exhibit a Poissonian distribution of spacings, while chaotic systems will instead be described by random matrix theory. An extensive study of the spectral statistics of the KDBH model was performed in Ref. [65], demonstrating that for $\kappa > 0.4$ it followed the Gaussian orthogonal ensemble [66], the same distribution as the bosonic SYK model [6].

The spectral distribution measures quantum chaos at timescales longer than $1/\delta$, where δ is the mean energy spacing. To make a complete comparison between the models, we must also consider their correspondence at short to intermediate times by calculating the spectral form factor (SFF), defined as $\mathrm{SFF}(t) = \left|\sum_j \exp\left(iE_j t\right)\right|^2 / D^2$, where D is the dimension of the Hilbert space, and E_j are the energies of the Hamiltonian (2). In order to extract the spectral distribution correctly, it is important to remove accidental symmetries, and block diagonalize the Hamiltonian in a particular symmetry sector [65]. We follow the same procedure here when calculating the SFF, and work in the zero momentum, reflection-symmetric subspace.

For many-body chaotic systems the SFF exhibits a particular structure: a non-universal drop at the Thouless time, followed by a linear ramp, which then transforms into a flat plateau $\mathrm{SFF}(t) \to 1/D$ for late times, $t > 1/\delta$. In Fig. 2, we show the SFF obtained for various combinations of (N, L), where N denotes the number of bosons in the system, and L is the number of sites. We observed that the form of the SFF did not depend on the value of κ, and so to reduce the size of fluctuations, we display the average of four different values of κ ($\kappa = 0.6, 0.7, 0.8, 0.9$). The data presented were further smoothened by computing a running 50-point average of the raw data. Scaling the SFF by a factor of D and the time coordinate by $1/D$ collapses the curves onto each other, displaying the required universal drop-ramp-plateau structure. From the graph it is clear that the Thouless time reduces as D increases, but the large non-universal fluctuations in the SFF in the vicinity of the transition to the ramp make it hard to measure this accurately. As a proxy, we define the *ramp time* as the time at which the scaled SFF first drops to a value of 0.1 of the plateau value, and plot this in the inset. This reveals that the ramp time scales quite accurately as $1/D$.

Note that reproducing the universal form of the SFF is a stricter condition than demonstrating the presence of quantum chaos via the spectral statistics. The Bose-Hubbard model, for example, displays GOE statistics for $U/J < 0.1$ [67], but its SFF does not exhibit the drop-ramp-plateau structure; see End Matter. This criterion was also used in Ref. [64] to determine when sparse SYK models failed to adequately reproduce SYK physics, the absence of the ramp corresponding to the loss of spectral rigidity and the transition to non-holographic behavior.

As a final point of comparison between the two models, we consider the out-of-time ordered correlation function (OTOC). The decay of this quantity measures the degree of "scrambling" in the system, that is, the delocalization of initially localized quantum information, and in particular the OTOC reveals the presence of quantum chaos at short timescales. The OTOC is a four-point correlation function of two local observables, and it is convenient to use a normalized version [68],

$$O(t) = \frac{\mathrm{Tr}\left[\rho\, W^\dagger(t) V^\dagger W(t) V\right]}{\mathrm{Tr}\left[\rho\, W(t)^2 V^\dagger V\right]} \,. \tag{5}$$

We take the system's temperature to be infinite ($\beta \to 0$) so that $\rho = I$ and all states enter the trace with equal weight. We have considerable freedom in our choice of the local operators V and W, as the scrambling dynamics should have a universal form, and we select the unitary operators $V = \exp\left[i\pi n_1\right]$ and $W = \exp\left[i\pi n_j\right]$, where n_j is the number operator acting on lattice site j. Since V and W take values of ± 1 when operating on a number state, they are a natural generalization of operators based on the fermionic number operator, and in principle can be measured by quantum gas microscopes [69] sensitive to the parity of the site occupation.

In Fig. 3(a), we show the OTOCs obtained for the BH model ($U = J$) for the three different spacings available: $d = 1$ (nearest-neighbor, i.e. W is evaluated at lattice site

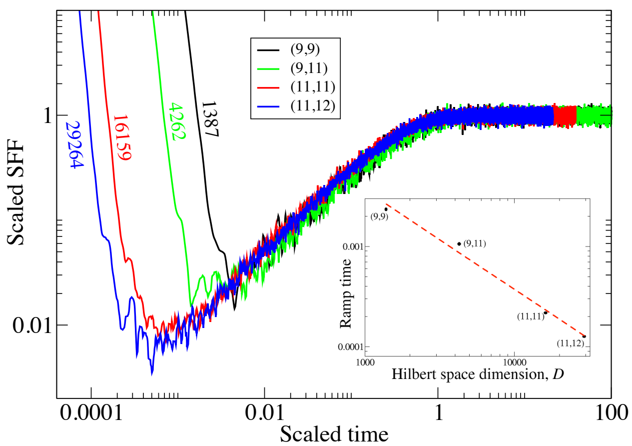

FIG. 2. Spectral form function (SFF) of the KDBH model for four different lattice sizes and bosons numbers; the notation (N, L) denotes N bosons on an L-site lattice. Multiplying the SFF by the dimension of the Hilbert space D, and scaling the time by $1/D$ collapses the curves to a universal form – an initial drop, then a linear ramp, followed by a constant plateau. Each curve is labeled by the corresponding values of D, and we see the ramp behavior occurring earlier as D increases. Inset - We define the ramp time as the time at which the scaled SFF falls to a value of 0.1. The red-dashed line drops as D^{-1}, and is included as a guide to the eye.

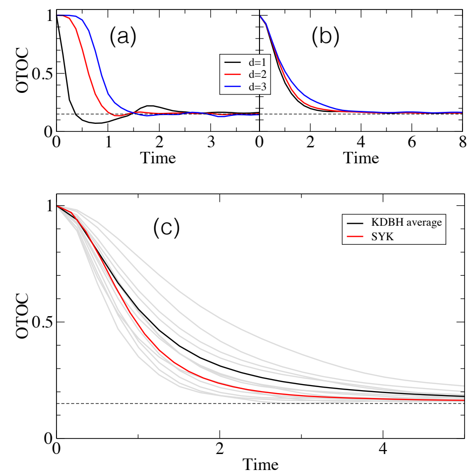

FIG. 3. (a) OTOCs for the BH model for 6 particles on a 6-site lattice with periodic boundary conditions. When the operators are separated by a single lattice spacing ($d = 1$) the OTOC rapidly decays to its asymptotic value. For larger spacings, $d = 2$ and $d = 3$ there is a delay until the OTOC begins its decay, corresponding to information spreading through the lattice at a finite speed. (b) As in (a) but for the KDBH model, with $\kappa = 0.8$. The OTOCs show no sign of a time delay, beginning their decay immediately. This indicates the lack of locality in this model. (c) Gray curves indicate the OTOCs obtained for the KDBH model for $\kappa = 0.6, 0.7, 0.8, 0.9$ for the three different separations. Their average, shown in black has the same form as the SYK OTOC, averaged over 25 random samples of $J_{ij;kl}$. To obtain quantitative agreement, the time coordinate of SYK data has been scaled by a factor of 9 (see text).

$j = 2$), $d = 2$ (next-nearest neighbor, $j = 3$) and the largest separation $d = 3$; these calculations are performed on a 6-site lattice with periodic boundary conditions. We can see that the $d = 1$ result rapidly decays to a small but non-zero value. However, for larger separations ($d = 2, 3$) there is a clear time delay before the decay occurs. This corresponds to information propagating through space at a finite rate, given by the butterfly velocity. In contrast to the SYK model, the BH chain thus exhibits spatial locality: an excitation made at a particular point propagates outwards in a light-cone structure.

This is very different to the behavior exhibited by the KDBH model, as shown in Fig. 3(b) for $\kappa = 0.8$. The three curves show a very similar decay, and they are no longer ordered by their value of separation d. This corroborates our expectation that the lattice connectivity seen in Fig. 1(b) substantially reduces the degree of locality from the BH case, due to the presence of effective long-range tunneling. The decay rate shows little dependence on the amplitude of the driving, and in Fig. 3(c) we plot the full set of OTOCs obtained for four values of κ. Averaging these 12 curves gives a result which agrees strikingly with that of the bosonic SYK model. The quantitative comparison depends on just one fitting parameter, a rescaling of time in the SYK model corresponding to the different energy scales of the two models arising from the distinct distributions of hopping amplitudes – the SYK model has a Gaussian distribution with unit variance, while the KDBH model has a narrower non-Gaussian form.

	SYK	Bose-Hubbard	KDBH
Long-range hopping	Yes	No	Yes
RMT statistics	Yes	Yes	Yes
Universal SFF	Yes	No	Yes
OTOC decay	Yes	No	Yes

TABLE I. Comparison of the considered models. The Bose-Hubbard model exhibits chaos in its spectral statistics, but otherwise does not exhibit any of the features of the SYK model. In contrast, the KDBH model indeed reproduces all of the four criteria commonly used to identify SYK physics.

Concluding remarks.— We summarize our comparative studies of the (bosonic) SYK, Bose-Hubbard and KDBH models in Table I. These results validate that SYK physics can be effectively realized using a practical periodic driving scheme.

As previously noted, the KDBH model can be implemented by modulating the Hubbard hopping amplitude J periodically in time, such that the average $\langle J(t) \rangle = 0$ over each driving period [58]. In practice, this can be achieved through a two-frequency drive: a lattice shaking of strength A and frequency ω_1 would renormalize the hopping strength according to a Bessel function $J_{\text{eff}} = \mathcal{J}_0(A/\omega_1)$ [26, 27, 70]; a modulation of the strength $A(t)$, at frequency $\omega_2 \ll \omega_1$, and in the vicinity of the Bessel-function root, would then realize the desired hopping modulation. This approach assumes a proper separation of energy scales, which is crucial in view of limiting heating, e.g. through inter-band processes [26]. Another promising direction relies on synthetic dimensions [71]. In this framework, one would induce and modulate couplings between a set of atomic internal states spanning a fictitious lattice. Finite-range interactions would be required along the synthetic dimension, which can be achieved through the scheme proposed in Ref. [72].

An interesting question concerns the experimental detection of SYK signatures in a Hubbard quantum simulator. An appealing approach would be to extract OTOCS by monitoring statistical correlations between randomized measurements [68] or through digital interferometric approaches [73]. Universal spectral signatures could be accessed by spectroscopy [74]. In principle, the long-range hopping amplitudes and fast scrambling could also be revealed by studying the dynamics of a mobile impurity immersed into the medium.

It would be worthwhile to investigate the potential effects of engineered disorder within our framework. As we show in the End Matter, breaking the translational symmetry of the KDBH model with a weak link provides a substantial improvement in the statistical distribution of the hopping amplitudes, and introducing other forms of disorder could also yield similar benefits. Finally, extending the framework to higher-dimensional systems should be straightforward and could open up intriguing avenues for exploration.

Acknowledgments.— We thank Antoine Georges, Subir Sachdev, Lauriane Chomaz, Oriana Diessel, Peter Schlagheck and Sylvain Nascimbene for discussions. This research was financially supported by the ERC Grant LATIS, the EOS project CHEQS and the Fondation ULB. CEC and FS were supported by the Spanish MICINN through grant no. PID2022-139288NB-I00.

[1] S. Sachdev and J. Ye, Gapless spin fluid ground state in a random, quantum Heisenberg magnet, Phys. Rev. Lett. **70**, 3339 (1993).

[2] A. Kitaev, A simple model of quantum holography, http://online.kitp.ucsb.edu/online/entangled15/kitaev/,http://online.kitp.ucsb.edu/online/entangled15/kitaev2/. Talks at KITP, April 7, 2015 and May 27, 2015.

[3] D. Chowdhury, A. Georges, O. Parcollet, and S. Sachdev, Sachdev-Ye-Kitaev models and beyond: Window into non-Fermi liquids, Rev. Mod. Phys. **94**, 035004 (2022).

[4] A. Georges, O. Parcollet, and S. Sachdev, Mean field theory of a quantum Heisenberg spin glass, Phys. Rev. Lett. **85**, 840 (2000).

[5] A. Georges, O. Parcollet, and S. Sachdev, Quantum fluctuations of a nearly critical heisenberg spin glass, Phys. Rev. B **63**, 134406 (2001).

[6] W. Fu and S. Sachdev, Numerical study of fermion and boson models with infinite-range random interactions, Phys. Rev. B **94**, 035135 (2016).

[7] C. L. Baldwin and B. Swingle, Quenched vs annealed: Glassiness from sk to syk, Phys. Rev. X **10**, 031026 (2020).

[8] B. Swingle and M. Winer, Bosonic model of quantum holography, Phys. Rev. B **109**, 094206 (2024).

[9] Y. Liu, A. Kulkarni, and S. Ryu, Dissipative dynamics and symmetry breaking in bosonic Sachdev-Ye-Kitaev Lindbladian (2025), arXiv:2508.04802 [quant-ph].

[10] A. Chen, R. Ilan, F. de Juan, D. I. Pikulin, and M. Franz, Quantum holography in a graphene flake with an irregular boundary, Phys. Rev. Lett. **121**, 036403 (2018).

[11] A. Chew, A. Essin, and J. Alicea, Approximating the Sachdev-Ye-Kitaev model with Majorana wires, Phys. Rev. B **96**, 121119 (2017).

[12] D. I. Pikulin and M. Franz, Black hole on a chip: Proposal for a physical realization of the Sachdev-Ye-Kitaev model in a solid-state system, Phys. Rev. X **7**, 031006 (2017).

[13] C. Wei and T. A. Sedrakyan, Optical lattice platform for the Sachdev-Ye-Kitaev model, Phys. Rev. A **103**, 013323 (2021).

[14] I. Danshita, M. Hanada, and M. Tezuka, Creating and probing the Sachdev-Ye-Kitaev model with ultracold gases: Towards experimental studies of quantum gravity, Progress of Theoretical and Experimental Physics **2017**, 083I01 (2017).

[15] T. Schuster, B. Kobrin, P. Gao, I. Cong, E. T. Khabiboulline, N. M. Linke, M. D. Lukin, C. Monroe, B. Yoshida, and N. Y. Yao, Many-body quantum teleportation via operator spreading in the traversable wormhole protocol, Phys. Rev. X **12**, 031013 (2022).

[16] P. Uhrich, S. Bandyopadhyay, N. Sauerwein, J. Sonner, J.-P. Brantut, and P. Hauke, A cavity quantum electrodynamics implementation of the Sachdev-Ye-Kitaev model (2023), arXiv:2303.11343 [quant-ph].

[17] R. Baumgartner, P. Pelliconi, S. Bandyopadhyay, F. Orsi, N. Sauerwein, P. Hauke, J.-P. Brantut, and J. Sonner, Quantum simulation of the Sachdev-Ye-Kitaev model using time-dependent disorder in optical cavities (2024), arXiv:2411.17802 [quant-ph].

[18] L. García-Álvarez, I. L. Egusquiza, L. Lamata, A. del Campo, J. Sonner, and E. Solano, Digital quantum simulation of minimal $\mathrm{AdS/CFT}$, Phys. Rev. Lett. **119**, 040501 (2017).

[19] R. Babbush, D. W. Berry, and H. Neven, Quantum simulation of the Sachdev-Ye-Kitaev model by asymmetric qubitization, Phys. Rev. A **99**, 040301 (2019).

[20] D. Jafferis, A. Zlokapa, J. D. Lykken, D. K. Kolchmeyer, S. I. Davis, N. Lauk, H. Neven, and M. Spiropulu, Traversable wormhole dynamics on a quantum processor, Nature **612**, 51 (2022).

[21] M. Asaduzzaman, R. G. Jha, and B. Sambasivam, Sachdev-Ye-Kitaev model on a noisy quantum computer, Phys. Rev. D **109**, 105002 (2024).

[22] T. A. Chowdhury, K. Yu, and R. S. Sufian, First measure-

ment of entanglement dynamics in the SYK model using quantum computers (2025), arXiv:2503.18580 [quant-ph].

[23] S. Blanes, F. Casas, J. Oteo, and J. Ros, The Magnus expansion and some of its applications, Physics Reports **470**, 151 (2009).

[24] N. Goldman and J. Dalibard, Periodically driven quantum systems: Effective Hamiltonians and engineered gauge fields, Phys. Rev. X **4**, 031027 (2014).

[25] M. Bukov, L. D'Alessio, and A. Polkovnikov, Universal high-frequency behavior of periodically driven systems: from dynamical stabilization to Floquet engineering, Advances in Physics **64**, 139 (2015), https://doi.org/10.1080/00018732.2015.1055918.

[26] A. Eckardt, Colloquium: Atomic quantum gases in periodically driven optical lattices, Rev. Mod. Phys. **89**, 011004 (2017).

[27] A. Zenesini, H. Lignier, D. Ciampini, O. Morsch, and E. Arimondo, Coherent control of dressed matter waves, Phys. Rev. Lett. **102**, 100403 (2009).

[28] A. Bermudez, T. Schaetz, and D. Porras, Synthetic gauge fields for vibrational excitations of trapped ions, Phys. Rev. Lett. **107**, 150501 (2011).

[29] A. R. Kolovsky, Creating artificial magnetic fields for cold atoms by photon-assisted tunneling, Europhysics Letters **93**, 20003 (2011).

[30] C. E. Creffield and F. Sols, Comment on "Creating artificial magnetic fields for cold atoms by photon-assisted tunneling" by Kolovsky A. R., Europhysics Letters **101**, 40001 (2013).

[31] J. Struck, C. Ölschläger, M. Weinberg, P. Hauke, J. Simonet, A. Eckardt, M. Lewenstein, K. Sengstock, and P. Windpassinger, Tunable gauge potential for neutral and spinless particles in driven optical lattices, Phys. Rev. Lett. **108**, 225304 (2012).

[32] P. Hauke, O. Tieleman, A. Celi, C. Ölschläger, J. Simonet, J. Struck, M. Weinberg, P. Windpassinger, K. Sengstock, M. Lewenstein, and A. Eckardt, Non-abelian gauge fields and topological insulators in shaken optical lattices, Phys. Rev. Lett. **109**, 145301 (2012).

[33] N. Goldman, J. Dalibard, M. Aidelsburger, and N. R. Cooper, Periodically driven quantum matter: The case of resonant modulations, Phys. Rev. A **91**, 033632 (2015).

[34] C. E. Creffield, G. Pieplow, F. Sols, and N. Goldman, Realization of uniform synthetic magnetic fields by periodically shaking an optical square lattice, New Journal of Physics **18**, 093013 (2016).

[35] N. Goldman, J. C. Budich, and P. Zoller, Topological quantum matter with ultracold gases in optical lattices, Nature Physics **12**, 639 (2016).

[36] N. R. Cooper, J. Dalibard, and I. B. Spielman, Topological bands for ultracold atoms, Rev. Mod. Phys. **91**, 015005 (2019).

[37] C. Weitenberg and J. Simonet, Tailoring quantum gases by Floquet engineering, Nature Physics **17**, 1342 (2021).

[38] R. Ma, M. E. Tai, P. M. Preiss, W. S. Bakr, J. Simon, and M. Greiner, Photon-assisted tunneling in a biased strongly correlated Bose gas, Phys. Rev. Lett. **107**, 095301 (2011).

[39] A. J. Daley and J. Simon, Effective three-body interactions via photon-assisted tunneling in an optical lattice, Phys. Rev. A **89**, 053619 (2014).

[40] M. Hafezi, P. Adhikari, and J. M. Taylor, Engineering three-body interaction and Pfaffian states in circuit QED systems, Phys. Rev. B **90**, 060503 (2014).

[41] C. H. Lee, W. W. Ho, B. Yang, J. Gong, and Z. Papić, Floquet mechanism for non-abelian fractional quantum Hall states, Phys. Rev. Lett. **121**, 237401 (2018).

[42] A. Rapp, X. Deng, and L. Santos, Ultracold lattice gases with periodically modulated interactions, Phys. Rev. Lett. **109**, 203005 (2012).

[43] M. D. Liberto, C. E. Creffield, G. I. Japaridze, and C. M. Smith, Quantum simulation of correlated-hopping models with fermions in optical lattices, Phys. Rev. A **89**, 013624 (2014).

[44] F. Meinert, M. J. Mark, K. Lauber, A. J. Daley, and H.-C. Nägerl, Floquet engineering of correlated tunneling in the Bose-Hubbard model with ultracold atoms, Phys. Rev. Lett. **116**, 205301 (2016).

[45] F. Görg, K. Sandholzer, J. Minguzzi, R. Desbuquois, M. Messer, and T. Esslinger, Realization of density-dependent Peierls phases to engineer quantized gauge fields coupled to ultracold matter, Nature Physics **15**, 1161 (2019).

[46] L. Barbiero, C. Schweizer, M. Aidelsburger, E. Demler, N. Goldman, and F. Grusdt, Coupling ultracold matter to dynamical gauge fields in optical lattices: From flux attachment to Z2 lattice gauge theories, Science Advances **5**, eaav7444 (2019).

[47] C. Schweizer, F. Grusdt, M. Berngruber, L. Barbiero, E. Demler, N. Goldman, I. Bloch, and M. Aidelsburger, Floquet approach to Z2 lattice gauge theories with ultracold atoms in optical lattices, Nature Physics **15**, 1168 (2019).

[48] H. Kamal, J. Kemp, Y.-C. He, Y. Fuji, M. Aidelsburger, P. Zoller, and N. Y. Yao, Floquet flux attachment in cold atomic systems, Phys. Rev. Lett. **133**, 163403 (2024).

[49] H. P. Zahn, V. P. Singh, M. N. Kosch, L. Asteria, L. Freystatzky, K. Sengstock, L. Mathey, and C. Weitenberg, Formation of spontaneous density-wave patterns in dc driven lattices, Phys. Rev. X **12**, 021014 (2022).

[50] N. Goldman, O. Diessel, L. Barbiero, M. Prüfer, M. Di Liberto, and L. Peralta Gavensky, Floquet-engineered nonlinearities and controllable pair-hopping processes: From optical Kerr cavities to correlated quantum matter, PRX Quantum **4**, 040327 (2023).

[51] A. Defossez, L. Vanderstraeten, L. Peralta Gavensky, and N. Goldman, Dynamic realization of Majorana zero modes in a particle-conserving ladder, Phys. Rev. Res. **7**, 023183 (2025).

[52] C.-L. Hung, A. González-Tudela, J. I. Cirac, and H. J. Kimble, Quantum spin dynamics with pairwise-tunable, long-range interactions, Proceedings of the National Academy of Sciences **113**, E4946 (2016).

[53] J. Choi, H. Zhou, H. S. Knowles, R. Landig, S. Choi, and M. D. Lukin, Robust dynamic Hamiltonian engineering of many-body spin systems, Phys. Rev. X **10**, 031002 (2020).

[54] S. Geier, N. Thaicharoen, C. Hainaut, T. Franz, A. Salzinger, A. Tebben, D. Grimshandl, G. Zürn, and M. Weidemüller, Floquet Hamiltonian engineering of an isolated many-body spin system, Science **374**, 1149 (2021).

[55] B.-Y. Sun, N. Goldman, M. Aidelsburger, and M. Bukov, Engineering and probing non-abelian chiral spin liquids using periodically driven ultracold atoms, PRX Quantum **4**, 020329 (2023).

[56] N. Nishad, A. Keselman, T. Lahaye, A. Browaeys, and

S. Tsesses, Quantum simulation of generic spin-exchange models in Floquet-engineered Rydberg-atom arrays, Phys. Rev. A **108**, 053318 (2023).

[57] H. Dehghani, M. Hafezi, and P. Ghaemi, Light-induced topological superconductivity via Floquet interaction engineering, Phys. Rev. Res. **3**, 023039 (2021).

[58] G. Pieplow, F. Sols, and C. E. Creffield, Generation of atypical hopping and interactions by kinetic driving, New Journal of Physics **20**, 073045 (2018).

[59] G. Pieplow, C. E. Creffield, and F. Sols, Protected cat states from kinetic driving of a boson gas, Phys. Rev. Res. **1**, 033013 (2019).

[60] J. Mateos, C. E. Creffield, and F. Sols, Superfluidity from correlations in driven boson systems, New Journal of Physics **25**, 063006 (2023).

[61] D. Jaksch, C. Bruder, J. I. Cirac, C. W. Gardiner, and P. Zoller, Cold bosonic atoms in optical lattices, Phys. Rev. Lett. **81**, 3108 (1998).

[62] M. Greiner, O. Mandel, T. Esslinger, T. W. Hänsch, and I. Bloch, Quantum phase transition from a superfluid to a Mott insulator in a gas of ultracold atoms, Nature **415**, 39 (2002).

[63] Y. Cao, Y.-N. Zhou, T.-T. Shi, and W. Zhang, Towards quantum simulation of Sachdev-Ye-Kitaev model, Science Bulletin **65**, 1170 (2020).

[64] P. Orman, H. Gharibyan, and J. Preskill, Quantum chaos in the sparse SYK model (2024), arXiv:2403.13884 [hep-th].

[65] J. Mateos, F. Sols, and C. Creffield, Spectral statistics of driven Bose-Hubbard models, Journal of Statistical Mechanics: Theory and Experiment **2024**, 063104 (2024).

[66] When the number of sites and the number of particles are both even, a hidden symmetry splits the distribution into being the sum of two GOEs. In this work we choose both parameters to be odd to consider just the single GOE case.

[67] C. Kollath, G. Roux, G. Biroli, and A. M. Läuchli, Statistical properties of the spectrum of the extended Bose-Hubbard model, Journal of Statistical Mechanics: Theory and Experiment **2010**, P08011 (2010).

[68] B. Vermersch, A. Elben, L. M. Sieberer, N. Y. Yao, and P. Zoller, Probing scrambling using statistical correlations between randomized measurements, Phys. Rev. X **9**, 021061 (2019).

[69] J. F. Sherson, C. Weitenberg, M. Endres, M. Cheneau, I. Bloch, and S. Kuhr, Single-atom-resolved fluorescence imaging of an atomic Mott insulator, Nature **467**, 68 (2010).

[70] P. K. Tien and J. P. Gordon, Multiphoton process observed in the interaction of microwave fields with the tunneling between superconductor films, Phys. Rev. **129**, 647 (1963).

[71] A. Celi, P. Massignan, J. Ruseckas, N. Goldman, I. B. Spielman, G. Juzeliūnas, and M. Lewenstein, Synthetic gauge fields in synthetic dimensions, Phys. Rev. Lett. **112**, 043001 (2014).

[72] L. Barbiero, L. Chomaz, S. Nascimbene, and N. Goldman, Bose-Hubbard physics in synthetic dimensions from interaction trotterization, Phys. Rev. Res. **2**, 043340 (2020).

[73] Google Quantum AI and Collaborators, Observation of constructive interference at the edge of quantum ergodicity, Nature **646**, 825 (2025).

[74] P. Roushan, C. Neill, J. Tangpanitanon, V. M. Bastidas, A. Megrant, R. Barends, Y. Chen, Z. Chen, B. Chiaro, A. Dunsworth, A. Fowler, B. Foxen, M. Giustina, E. Jeffrey, J. Kelly, E. Lucero, J. Mutus, M. Neeley, C. Quintana, D. Sank, A. Vainsencher, J. Wenner, T. White, H. Neven, D. G. Angelakis, and J. Martinis, Spectroscopic signatures of localization with interacting photons in superconducting qubits, Science **358**, 1175 (2017).

End Matter

Derivation of the effective Hamiltonian for the driven Bose-Hubbard system – To illustrate the technique, we first consider the standard BH model (1),

$$H = -J \sum_j \left(b^\dagger_{j+1} b_j + \text{H.c.} \right) + U \sum_j b^\dagger_j b^\dagger_j b_j b_j \ , \qquad \text{(EM1)}$$

where j labels the lattice sites, and we take periodic boundary conditions. We now Fourier transform this Hamiltonian to momentum space, and allow the hopping to vary periodically in time, $J(t) = J_0 \cos \omega t$ to obtain

$$\begin{aligned} H(t) &= -2J_0 \cos \omega t \sum_k \cos k \ b^\dagger_k b_k \\ &+ \frac{U}{2L} \sum_{k_1,k_2,k_3,k_4} \delta_{k_1+k_2,k_3+k_4} b^\dagger_{k_4} b^\dagger_{k_3} b_{k_2} b_{k_1} \ , \end{aligned}$$

where the δ-function enforces quasimomentum conservation, and the summations are taken over the first Brillouin zone. Clearly when time-averaged over one period of the driving, the first term in this equation vanishes, meaning that, as in the SYK model itself, single-particle hopping terms are absent.

To ensure convergence of the high-frequency expansion [24, 25, 33], we now transform to the interaction picture, $H'(t) = i\dot{W}(t) W^\dagger(t) + W(t) H(t) W^\dagger(t)$, where the unitary operator $W(t)$ is defined as,

$$W(t) = \exp \left[-2i\kappa \sin \omega t \sum_k \cos k \ b^\dagger_k b_k \right] , \qquad \text{(EM2)}$$

and $\kappa = J_0/\omega$. To perform this transformation it is advantageous to define the operator

$$\begin{aligned} f(\lambda) &= e^{-i\lambda \cos k \ b^\dagger_k b_k} b^\dagger_{k_4} b^\dagger_{k_3} b_{k_2} b_{k_1} e^{i\lambda \cos k \ b^\dagger_k b_k} \\ &= U(\lambda) b^\dagger_{k_4} b^\dagger_{k_3} b_{k_2} b_{k_1} U^\dagger(\lambda) \ . \end{aligned} \qquad \text{(EM3)}$$

In order to obtain $f(\lambda)$ in closed form, we first differentiate it with respect to λ,

$$\partial_\lambda f(\lambda) = i \cos k U(\lambda) \left[b^\dagger_{k_4} b^\dagger_{k_3} b_{k_2} b_{k_1}, b^\dagger_k b_k \right] U^\dagger(\lambda) \ . \qquad \text{(EM4)}$$

As shown in Ref. [58], this differential equation has the solution

$$f(\lambda) = e^{i\lambda \cos k \left(\delta_{kk_1} + \delta_{kk_2} - \delta_{kk_3} - \delta_{kk_4} \right)} b^\dagger_{k_4} b^\dagger_{k_3} b_{k_2} b_{k_1} \ , \qquad \text{(EM5)}$$

which enables the transformed Hamiltonian to be expressed as

$$H'(t) = \frac{U}{2L} \sum_{k_1,k_2,k_3,k_4} \delta_{k_1+k_2,k_3+k_4} e^{2i\kappa \sin\omega t(\cos k_1 + \cos k_2 - \cos k_3 - \cos k_4)} b^\dagger_{k_4} b^\dagger_{k_3} b_{k_2} b_{k_1} \ . \tag{EM6}$$

Considering the high-frequency regime $\omega \gg U$, we calculate the lowest-order term in the Magnus expansion [23–26] by time-averaging Eq. (EM6) over one driving period. Making use of the Jacobi-Anger expansion, this gives the effective Hamiltonian

$$H_{\text{eff}} = \frac{1}{T}\int_0^T dt H'(t) = \frac{U}{2L} \sum_{k_1,k_2,k_3,k_4} \delta_{k_1+k_2,k_3+k_4} \mathcal{J}_0 \left(2\kappa \left[\cos k_1 + \cos k_2 - \cos k_3 - \cos k_4\right]\right) \ b^\dagger_{k_4} b^\dagger_{k_3} b_{k_2} b_{k_1} \ , \tag{EM7}$$

where $\mathcal{J}_0$ is the Bessel function of zeroth order. Transforming this result back to real space yields the KDBH model,

$$H_{\text{KDBH}} = U \sum_{i,j,k,l} Q_{ijkl} b^\dagger_i b^\dagger_j b_k b_l \tag{EM8}$$

where the hopping amplitudes are given by,

$$Q_{ijkl} = \frac{1}{2L^3} \sum_{k_1,k_2,k_4} e^{i(k_1(j-l)+k_2(j-k)+k_4(i-j))} \mathcal{J}_0 \left[2\kappa \left(\cos k_1 + \cos k_2 - \cos\left(k_1+k_2-k_4\right) - \cos k_4\right)\right] \ . \tag{EM9}$$

We note that higher-order terms in the effective Hamiltonian would correspond to many-body interactions (beyond two-body interactions). These are neglected in the present study, which assumes a high frequency regime $\omega \gg U$.

Breaking translational symmetry – As can be seen in Fig. 1(b), the distribution of the Q_{ijkl} is far from Gaussian, and also exhibits various gaps. We attribute this feature to the translational invariance of the model, which leads to the spatial structures displayed in Eq. (EM9). To explore this effect, we now introduce a small defect that explicitly breaks translational symmetry: following Ref. [60], we obtain the Q amplitudes when one of the hoppings in the BH model differs from the others by ϵ. We show the result in Fig. EM1 for $\epsilon = 0.001$. We find that this slight breaking of translational invariance is enough to refine the distribution of the Q amplitudes, bringing it into closer alignment with the Gaussian form characteristic of the SYK model.

Derivation of the effective Hamiltonian for a driven Fermi-Hubbard system – The derivation for a fermionic system proceeds in much the same way as above. We must consider a different starting Hamiltonian, however, as the Hubbard interaction written in Eq. EM1 would identically vanish. Accordingly we introduce a Hubbard-type model with nearest-neighbor interactions

$$H = -J \sum_j \left(c^\dagger_{j+1} c_j + \text{H.c.}\right) + U \sum_j c^\dagger_j c^\dagger_{j+1} c_j c_{j+1} \ , \tag{EM10}$$

where $c_j / c^\dagger_j$ are spinless fermion operators.

Following the same procedure as before we obtain a very similar form for the $f(\lambda)$ operator, only differing from (EM3) by a momentum-dependent phase

$$f(\lambda) = e^{i(k_4 - k_2)} \ U(\lambda) c^\dagger_{k_4} c^\dagger_{k_3} c_{k_2} c_{k_1} U^\dagger(\lambda) \ . \tag{EM11}$$

Noting that the commutator in Eq. EM4 does not depend upon the particle statistics, we can again obtain a closed form solution for $f(\lambda)$, and hence obtain the hopping amplitudes for this model

$$Q_{ijkl} = \frac{1}{2L^3} \sum_{k_1,k_2,k_4} e^{i(k_1(j-l)+k_2(j-k-1)+k_4(i-j+1))} \mathcal{J}_0 \left[2\kappa \left(\cos k_1 + \cos k_2 - \cos\left(k_1+k_2-k_4\right) - \cos k_4\right)\right] \ . \tag{EM12}$$

Comparing the expressions for Q_{ijkl} in the two models reveals their strong similarity, and in fact (EM12) can be mapped to (EM9) by making the substitutions $i \to i-1, \ k \to k-1$. Consequently the distribution of Q_{ijkl} in the two models is identical, the difference being that Q_{ijkl} labels different processes in each case.

We emphasise that the amplitudes do not depend on the statistics of the particle – the same result (EM12) is obtained for both bosons and spinless fermions. Accordingly we believe that kinetically-driven Hubbard models of both bosonic and fermionic type will permit the simulation of the corresponding SYK Hamiltonians.

SFF of the BH model – The SFF of the KDBH model displays the universal form expected of chaotic systems, consisting of a rapid drop up to the Thouless time, followed by a linear ramp, and finally a plateau at long times. This behavior can be clearly seen in Fig. EM2a, where we plot a typical example, the SFF for a $(11, 11)$ system at $\kappa = 0.8$.

As we note in the text and in Table I, the BH model does not follow this form. In fig. EM2b we show the SFF for a weakly interacting BH model, which after the initial fall first goes through a preliminary plateau, before then showing the ramp and final plateau at longer times. In contrast to the KDBH and SYK models, the BH model thus only manifests chaos at long time scales, the initial plateau possibly indicating a pre-thermalisation regime where the Hilbert space of the system is not fully explored.

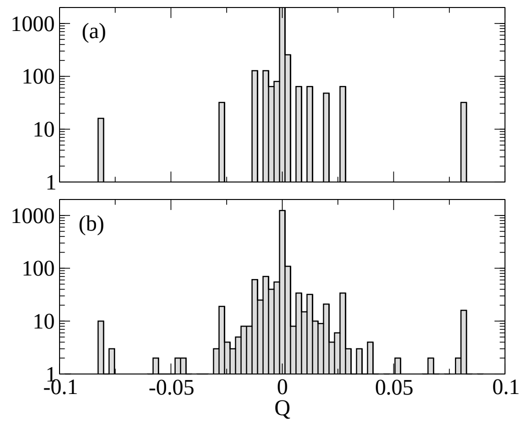

FIG. EM1. Distributions of the Q amplitudes in an 8-site KDBH model for $\kappa = 0.6$. (a) Clean system: as seen previously, the distribution is non-Gaussian and contains several gaps. (b) Introducing a weak link in the parent BH Hamiltonian with $J = (J - \epsilon)$ produces a distribution much closer to the target Gaussian form.

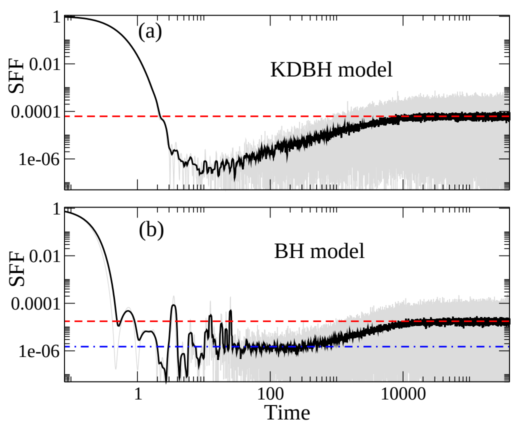

FIG. EM2. (a) The SFF for the KDBH model ($\kappa = 0.8$ and $(N, L) = (11, 11)$) follows the universal form: a sharp decay at the Thouless time, followed by a linear ramp before finally reaching a plateau. The gray curve shows the raw data, the black line is obtained by a 50-point running average to smoothen the oscillations. (b) In contrast, the SFF for the BH model ($U = 0.2J$ and $(12, 12)$) does not have the universal form. Following the initial decay, the SFF first oscillates about a constant value, before going through the ramp-plateau behavior at a much later time. Red dashed lines indicate the value of D^{-1} (where D is the dimension of the Hilbert space); the blue dot-dashed line is a guide to the eye indicating the first plateau of the BH model.